Inorganic Chemistry

Article

pubs.acs.org/IC

Electrochemiluminescence Properties of $[Pt_2Ag_4(C{\equiv}CC_6H_4R)_8]_n$ (R = CH_3, n = 1; R = H, n = 1 and 2) with Amine (TPrA and DBAE) as the Coreactant and Determination of Sudan I

Qiao-Hua Wei,*[,†,‡] Li-Jing Han,[†] Yi Jiang,[†] Xiao-Xia Lin,[†] Ya-Nan Duan,[†] and Guo-Nan Chen*[,†]

[†]Ministry of Education, Fujian Provincial Key Lab of Analysis and Detection for Food Safety, and Department of Chemistry, Fuzhou University, Fuzhou 3500108, China

[‡]Beijing Synchrotron Radiation Laboratory, Institute of High Energy Physics, The Chinese Academy of Sciences, Beijing 100039, China

Supporting Information

ABSTRACT: Two hexanuclear clusters, $[Pt_2Ag_4(C{\equiv}CC_6H_4R)_8]$ (R = CH_3, **1**; R = H, **2**), together with dimer $[Pt_2Ag_4(C{\equiv}CC_6H_5)_8]_2$ (**3**), have been synthesized and characterized by elemental analyses, electrospray ionization mass spectrometry, and ^{1}H NMR spectroscopy and by X-ray crystallography for **1** and **3**. A considerable enhancement of photoluminescence (PL) and a notable red shift in the emission maximum of **1** (λ_{max} 600 nm) relative to **2** (λ_{max} 545 nm) are observed. Electrogenerated chemiluminescence (ECL) of **1** and **2** in the absence or presence of coreactant tri-*n*-propylamine (TPrA) or 2-(dibutylamino)ethanol (DBAE) at different working electrodes in different solvents (CH_2Cl_2, CH_2ClCH_2Cl, or CH_3CN) has been studied. The ECL spectra are identical with the PL spectra, indicating that ECL emissions are also due to a MLM′CT [Pt(d)/π ($C{\equiv}CC_6H_4$R-4) → Pt(p_z)/Ag(sp)/π* ($C{\equiv}CC_6H_4$R-4)] state modified by Pt···Ag and Ag···Ag contacts. ECL of **1**- and **2**/amine systems in CH_2ClCH_2Cl was produced at the potentials of 1.14−1.19 V vs SCE, notably negatively shifted by about 0.38 V compared to those of the $Ru(bpy)_3^{2+}$/amine system. In all cases, ECL quantum efficiencies of **2** are higher than those of **1** and on the same order of magnitude as that of the $[Ru(bpy)_3](PF_6)_2$/amine system. It is noted that Sudan I tends to decrease the ECL intensity of the **1**/DBAE system in CH_2ClCH_2Cl at a platinum working electrode. A new ECL method for the determination of Sudan I was developed with a linear range of 2.5×10^{-5}−1.0×10^{-3} M and a detection limit of 8.0×10^{-6} M based on 3 times the ratio of signal-to-noise.

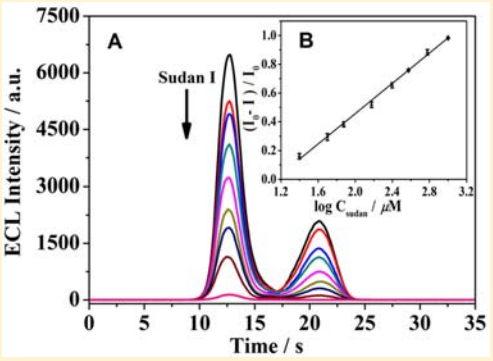

INTRODUCTION

Electrogenerated chemiluminescence (ECL), also called electrochemiluminescence, is a kind of luminescence produced by electrochemical reactions. ECL has become a powerful analytical technique in the past decades because of its high versatility, simplified optical setup, good temporal and spatial control, fast sample analysis, and a very low background signal.[1] Among the ECL systems, $[Ru(bpy)_3]^{2+}$ is one of the most studied objects for its high ECL sensitivity and high stability, which has led to widespread application of ECL in food, biosensors, immunoassays, and environmental pollutant testing.[2−6] With the increasing application of ECL, it is of considerable interest to develop new and efficient ECL systems that are different from $[Ru(bpy)_3]^{2+}$ systems.[1,7,8]

Square-planar platinum(II) alkynyl complexes, especially platinum(II) to metal(I) [metal = silver(I), copper(I), and gold(I)] heterometallic alkynyl complexes, have been extensively studied in the last few decades, with a focus on their chemical reactivity, structural topologies, and photoluminescence (PL) properties.[9−12] In contrast, ECL properties of platinum(II) alkynyl complexes are extremely rare. To our best knowledge, this is only one case of the ECL study of mononuclear platinum(II) alkynyl terpyridine complexes, [Pt(^{t}Bu$_3$tpy)(C≡CC$_6$H$_4$-4-carbazole-9](OTf) (^{t}Bu$_3$tpy = 4,4′,4′′-tri-*tert*-butyl-2,2′:6′,2′′-terpyridine), using $S_2O_8^{2-}$ as the coreactant.[8b] Because platinum(II) to metal(I) [metal = silver(I), copper(I), gold(I)] heterometallic alkynyl complexes exhibit strong PL in solution, it is suggested that they may also function as ECL luminophores.

Sudan I (1-phenylazo-2-naphthol), one of the most frequently used Sudan dyes, has been widely used in many fields, such as petroleum, shoe polishes, and textile colorants. It has been reported that it may pose an increased risk of cancer for humans.[13] The use of Sudan I in foods is now strictly forbidden worldwide according to both the Food Standards Agency and the European Union.[14] Consequently, the development of highly effective and practicable methods for the selective determination of Sudan I in foodstuffs is urgently required. Until now, the most widely used method for Sudan

Received: July 30, 2012
Published: September 27, 2012

   dx.doi.org/10.1021/ic3016657 | *Inorg. Chem.* 2012, 51, 11117−11125

dyes is liquid chromatography associated with different detectors, such as ultraviolet (UV),[15] mass spectrometry (MS),[16] diode array detection,[17] and chemiluminescence (CL).[18] Besides, many other methods have been developed, for example, electrochemical sensors,[19] molecularly imprinted polymers,[20] plasmon resonance light scattering,[21] and enzyme-linked immunosorbent assays.[22] To our best knowledge, no ECL method has been reported for the determination of Sudan I.

Several years ago, several hexanuclear clusters $[Pt_2Ag_4(C{\equiv}CR)_8]$ (R = Bu^t, C_6H_5, C_6H_4OMe-3, C_6H_4CN-4, C_6H_4CF-4, C_5H_4N-4, $C{\equiv}CC{\equiv}CC_6H_4CH_3$-4) were synthesized by the reaction of $PtCl_2(tht)_2$ and $(AgC{\equiv}CR)_n$ reported by Forniés et al.[23] or by the reaction of $[NBu_4]_2[Pt(C{\equiv}CC_6H_4R\text{-}4)_4]$ and Ag^+ reported by Yam et al.[24] It was found that clusters $[Pt_2Ag_4(C{\equiv}CR)_8]$ with phenylethynyl derivatives exhibited rich polymorphism and interesting PL properties. In this contribution, two monomers $[Pt_2Ag_4(C{\equiv}CC_6H_4R)_8]$ (R = CH_3, **1**; R = H, **2**), together with dimer $[Pt_2Ag_4(C{\equiv}CC_6H_5)_8]_2$ (**3**), were prepared using $[NBu_4]_2[Pt(C{\equiv}CC_6H_4R\text{-}4)_4]$ and $[Ag_2(\mu\text{-dppy})_2](ClO_4)_2$ [dppy = 2-(diphenylphosphino)-pyridyl] as building blocks and characterized by elemental analyses, electrospray ionization mass spectrometry (ESI-MS), and ^1H NMR spectroscopy and by X-ray crystallography for **1** and **3**. Their PL properties and electrochemical and ECL characteristics in the absence/presence of coreactant tri-*n*-propylamine (TPrA) or 2-(dibutylamino)ethanol (DBAE) at different working electrodes in different solvents (CH_2Cl_2, CH_2ClCH_2Cl, or CH_3CN) were extensively evaluated. The possible ECL mechanism of **1**- and **2**/TPrA systems was proposed. A new ECL method for the determination of Sudan I was developed, based on the fact that Sudan I decreases the ECL intensity of the complex **1**/DBAE system in CH_2ClCH_2Cl solution, with a linear range between 2.5×10^{-5} and 1.0×10^{-3} M and a detection limit of 8.0×10^{-6} M based on 3 times the ratio of signal-to-noise.

EXPERIMENTAL SECTION

Materials and Reagents. The reactions were carried out under a dry nitrogen atmosphere using Schlenk techniques. The solvents were purified and distilled by standard procedures prior to use. The ligands 2- (diphenylphosphino)pyridyl (dppy) and tetrabutylammonium hexafluorophosphate (Bu_4NPF_6) were purchased from Alfa Chemical Co. Ltd., China. Phenylacetylene ($HC{\equiv}CC_6H_5$) and 4-methylphenylacetylene ($HC{\equiv}CC_6H_4CH_3$-4) were obtained from Acros Organics. Coreactant tri-*n*-propylamine (TPrA) and 2-(dibutylamino)-ethanol (DBAE) were obtained from Aldrich. $[NBu_4]_2[Pt(C{\equiv}CC_6H_4R\text{-}4)_4]$ (R = H, CH_3),[23,24] and $[Ag_2(\mu\text{-dppy})_2](ClO_4)_2$[25] were prepared by literature procedures.

*$[Pt_2Ag_4(C{\equiv}CC_6H_4CH_3\text{-}4)_8]$ (**1**).* To a dichloromethane (100 mL) solution of $[NBu_4]_2[Pt(C{\equiv}CC_6H_4CH_3)_4]$ (296.6 mg, 0.26 mmol) was added $[Ag_2(\mu\text{-dppy})_2](ClO_4)_2$ (80.0 mg, 0.085 mmol). The resulting mixture was stirred for 24 h to give an orange solution, which was concentrated under reduced pressure. The orange crude products were purified by a silica gel (100−200 mesh) column chromatograph using dichloromethane/petroleum ether (1:1, v/v) as the eluent, and the first orange band was collected. Further purification was achieved by the slow diffusion of diethyl ether vapor into its concentrated dichloromethane solution to afford orange crystals. Yield: 210 mg (93%). Anal. Calcd for $C_{72}H_{56}Ag_4Pt_2$: C, 49.62; H, 3.24. Found: C, 49.65; H, 2.97. ESI-MS [*m*/*z* (%)]: 1636.0 (100) $[Pt_2Ag_3(C{\equiv}CC_6H_4CH_3\text{-}4)_8]^-$. IR (KBr, ν): 2049 cm^{-1} (m, C≡C). ^1H NMR (400.1 MHz, $CDCl_3$, ppm): δ 7.27 (d, *J* = 8.8 Hz, 16H), 6.94 (d, *J* = 8.0 Hz, 16H), 2.33 (s, 24H, CH_3).

*$[Pt_2Ag_4(C{\equiv}CC_6H_5)_8]_n$ (n = 1, **2**; n = 2, **3**).* The same synthetic procedure as that of **1** was employed by the reaction of $[Ag_2(\mu\text{-dppy})_2](ClO_4)_2$ (69.8 mg, 0.07 mmol) with $[NBu_4]_2[Pt(C{\equiv}CC_6H_5)_4]$ (241 mg, 0.22 mmol). The resulting mixture was stirred for 24 h to give a yellow solution, which was concentrated under reduced pressure. The yellow crude products were purified by a silica gel (100−200 mesh) column chromatograph using dichloromethane/petroleum ether (1:1, v/v) as the eluent, and a second yellow band was collected. Further purification was achieved by the slow diffusion of diethyl ether or petroleum ether vapor into its concentrated dichloromethane solution to afford yellow and red crystals.

*$[Pt_2Ag_4(C{\equiv}CC_6H_5)_8]$ (**2**).* Yield: 120 mg (67%). Anal. Calcd for $C_{64}H_{40}Ag_4Pt_2$: C, 47.14; H, 2.47. Found: C, 47.25; H, 2.16. ESI-MS [*m*/*z* (%)]:1523.4 (100) $[Pt_2Ag_3(C{\equiv}CC_6H_5)_8]^-$. IR (KBr, ν): 2040 cm^{-1} (m, C≡C). ^1H NMR (400.1 MHz, $CDCl_3$, ppm): δ 7.40 (d, *J* = 7.2 Hz, 16H), 7.23 (t, *J* = 7.6 Hz, 8H), 7.15 (t, *J* = 7.6 Hz, 16H).

*$[Pt_2Ag_4(C{\equiv}CC_6H_5)_8]_2$ (**3**).* Yield: 32 mg (28%). Anal. Calcd for $C_{128}H_{80}Ag_8Pt_4$: C, 47.14; H, 2.47. Found: C, 47.23; H, 2.40. ESI-MS [*m*/*z* (%)]: 1523.4 (100) $[Pt_2Ag_3(C{\equiv}CC_6H_5)_8]^-$. IR (KBr, ν): 2047 cm^{-1} (m, C≡C). ^1H NMR (400.1 MHz, $CDCl_3$, ppm): δ 7.40 (d, *J* = 6.8 Hz, 32H), 7.23 (t, *J* = 8.8 Hz, 16H), 7.15 (t, *J* = 7.6 Hz, 32H).

Crystal Structural Determination. Crystal **1** or **3** coated with epoxy resin was measured on a Mar CCD 165 nm diffractometer by the oscillation scan technique at 193 K using the Beijing Synchrotron Radiation Facility with a 3W1A beam (λ = 0.71073 Å). The cell refinement and data reduction were computed using the *HKL2000* software. Absorption correction was carried out based on spherical harmonics expansion of the absorption surface using the *HKL2000* software.[26a] The structure was solved by direct methods, and the heavy atoms were located from E-map. The remaining non-hydrogen atoms were determined from successive difference Fourier syntheses. All non-hydrogen atoms were refined anisotropically except those mentioned otherwise, and the hydrogen atoms of crystal **1** were generated geometrically with isotropic thermal parameters. The carbon atoms of the benzene ring in crystal **3** were disordered, and therefore the hydrogen atoms on the benzene ring were not added. The structure was refined on F^2 by full-matrix least-squares methods using the *SHELXTL-97* program package.[26b] The crystallographic parameters and details for data collections and refinements of crystals **1** and **3** are summarized in Table S1 in the Supporting Information. Full crystallographic data are provided in the CIF file.

Physical Measurements. IR spectra were recorded on a Perkin-Elmer 2000 FT-IR spectrophotometer with KBr pellets. Elemental analyses (C and H) were carried out on an Elementar Vario MICRO automatic instrument, and negative-ion ESI-MS spectra were performed on a Thermo Finnigan DECAX-3000 LCQ mass spectrometer using dichloromethane/methanol or acetonitrile/methanol as the mobile phase at the Fujian Institute of Research on the Structure of Matter, The Chinese Academy of Sciences. ^1H NMR spectra, with chemical shifts reported relative to tetramethylsilane, were recorded on a Bruker AVANCE 400 MHz spectrometer. UV−vis absorption spectra were measured on a Perkin-Elmer Lambda 750 UV−vis spectrometer. Steady-state emission and excitation spectra at room temperature were recorded on an Edinburgh Analytical Instrument (FLS900 fluorescence spectrometer). Emission lifetimes were determined on an Edinburgh Analytical Instrument (FLS900 fluorescence spectrometer) with a light-emitting diode lamp (405 nm) and analyzed by the use of a program for exponential fits. The luminescence quantum yield of the sample was determined according to

$$\Phi_s = \Phi_r(B_r/B_s)(n_s/n_r)^2(D_s/D_r) \quad (1)$$

where the subscripts s and r refer to the sample and reference solutions, respectively, and $B = 1 - 10^{-AL}$. *A* is the absorbance at the excitation wavelength, *L* is the path length, *n* is the refractive index of the solvent, and *D* is the integrated emission intensity. A degassed ethanol solution of Rhodamine 6G (Φ_{em} = 0.95)[27] and a degassed aqueous solution of $[Ru(bpy)_3]Cl_2$ (Φ_{em}= 0.042)[28] were used as references.

dx.doi.org/10.1021/ic3016657 | Inorg. Chem. 2012, 51, 11117−11125

Electrochemistry and ECL Measurements. The electrochemical and ECL properties of **1** and **2** in different solutions (CH_2Cl_2, $ClCH_2CH_2Cl$, or CH_3CN) were studied at room temperature using a system made in our laboratory,[29] consisting of a BPCL Ultra-Weak CL analyzer controlled by a personal computer (Institute of Biophysics, The Chinese Academy of Sciences) in conjunction with a CHI model 1210 electrochemical analyzer (Shanghai Chenghua Instrument Co., China). A three-electrode system was employed with platinum wire as the auxiliary electrode, Ag/Ag^+ as the reference electrode, and a platinum disk (Pt; 2 mm diameter), glass carbon (GC; 3 mm diameter), or gold (Au; 2 mm diameter) as the working electrode. The working electrodes were polished with 0.3 and 0.05 μm alumina slurry to obtain a mirror surface and then solicited and thoroughly rinsed with ultrapure deionized water. To eliminate the influence of oxygen, all solutions were deaerated by bubbling of high-purity (99.995%) nitrogen, and a constant flow of nitrogen was maintained over the solution during the measurements. The ECL signals were measured with a photomultiplier tube with a voltage of −800 V installed under the electrochemical cell. All potentials reported were against the SCE reference with the argotic system using ferrocene as an internal standard (E°_{Fc/Fc^+} = 0.424 V vs SCE).[30] The ECL quantum efficiencies of the **1**- and **2**/amine coreactant systems in CH_2ClCH_2Cl solution were measured using $[Ru(bpy)_3](PF_6)_2$ (φ°_{ECL} = 1) as the standard.[31]

RESULTS AND DISCUSSION

Synthesis and Characterization. Compounds **1**−**3** were prepared by the self-assembly reaction of $[Ag_2(\mu\text{-dppy})_2](ClO_4)_2$ with 3 equiv of $[NBu_4]_2[Pt(C{\equiv}CC_6H_4R\text{-}4)_4]$ (R = H, CH_3) in dichloromethane solutions. It is obvious that the phosphine ligands (dppy) were not involved in the reaction because of competition from alkynyl ligands. The subsequent diffusion of diethyl or petroleum ether into the dichloromethane solutions afforded monomer crystals $[Pt_2Ag_4(C{\equiv}CC_6H_4R\text{-}4)_8]$ (R = CH_3, **1**; R = H, **2**) and red dimer crystals **3**. Interestingly, it has been found that the diffusion solvent plays an important role in the formation of the products for the $C{\equiv}CC_6H_5$ ligand. The diffusion of diethyl ether vapor into their concentrated dichloromethane solutions afforded yellow monomer crystals **2** in high yields, while using petroleum ether as the diffusion solvent gave red dimer crystals **3** in high yields, as confirmed by analytical and X-ray crystallographic data. However, only orange monomer crystals **1** were obtained regardless of what diffusion solvent was used.

Crystals **1**−**3** were satisfactorily characterized by ESI-MS, ^1H NMR spectroscopy, elemental analyses, and IR spectroscopy. The IR spectra of compounds **1**−**3** all display one weak ν ($C{\equiv}C$) stretching vibration in the range of 2040−2049 cm^{-1}, which is shifted to lower frequency in relation to that of the homoleptic precursor $[NBu_4]_2[Pt(C{\equiv}CC_6H_4R\text{-}4)_4]$ (R = H, CH_3; 2077 and 2081 cm^{-1}), consistent with the bonding mode [μ-$\eta^1(\sigma)$ and $\eta^2(\pi)$] of the $C{\equiv}CC_6H_4R$-4 ligands.

Crystal Structures. It was reported that Forniés et al.[23a] tried many attempts at a complete X-ray study on the red dimer crystal **3**, but the crystal data were not good enough for a complete X-ray study. They only confirmed that two clusters $[Pt_2Ag_4(C{\equiv}CC_6H_5)_8]$ were linked by a Pt···Pt contact of 3.221(2) Å. Fortunately, crystals **1** and **3** were successfully characterized on a Mar CCD 165 nm diffractometer using the Beijing Synchrotron Radiation Facility with the 3W1A beam in this paper. Select bonding parameters of **1** and **3** are listed in Table S2 in the Supporting Information. Two crystallographically independent molecules A and B but with similar structural details were also found in **1**, compared with other reported clusters $[Pt_2Ag_4(C{\equiv}CR)_8]$ (R = Bu^t, C_6H_5, C_6H_4OMe-3, C_6H_4CN-4, $C_6H_4CF_3$-4, C_5H_4N-4, $C{\equiv}CC{\equiv}CC_6H_4CH_3$-4).[23,24] An ORTEP drawing of the molecule A structure of **1** is shown in Figure 1. The basic skeleton of **1**

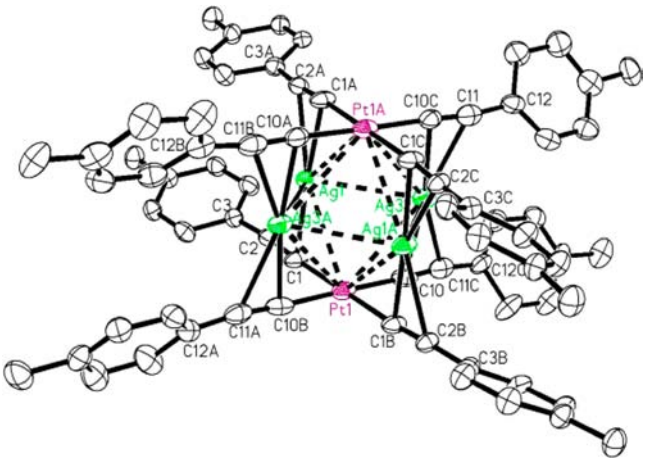

Figure 1. ORTEP view of **1** (molecule A) with 30% thermal ellipsoids.

exhibits a distorted octahedral geometry of the metal centers with the platinum atoms in a mutually trans disposition and the four silver atoms in the equatorial plane, which is similar to the other reported hexanuclear clusters $[Pt_2Ag_4(C{\equiv}CR)_8]$ (R = Bu^t, C_6H_5, C_6H_4OMe-3, C_6H_4CN-4, $C_6H_4CF_3$-4, C_5H_4N-4, $C{\equiv}CC{\equiv}CC_6H_4CH_3$-4).[23,24] The Pt···Ag distances are in the range of 3.0535(7)−3.1558 (9) Å and shorter than the sum of the van der Waals radii (3.45 Å), demonstrating the presence of strong Pt−Ag bonding interactions. The strong Ag−Ag bonding interactions are also found with Ag···Ag distances of 3.0689(10) and 3.0992(8) Å. All acetylides adopt a μ-η^1:η^2 bonding mode, bound to the platinum(II) and silver(I) centers. The bond distances of Pt−C are in the range of 2.003(10)−2.041(7) Å, compared to those found in the platinum(II)−silver(I) heterometallic alkynyl cluster.[23,24,32,33] It is obvious that the Ag−C π bonds are asymmetric, with Ag−C_α distances shorter than Ag−C_β bonds (Δ = 0.168−0.195 Å), and comparable to those found in related silver(I)−π bond alkynyl bridging complexes.[23,24,32,33]

The dimer **3** crystallizes in the tetragonal geometry of space group *P4/nnc* with two clusters **2** linked by a Pt···Pt contact of 3.2119(17) Å (shown in Figure 2), which is identical within experimental error to the analogous distance reported by Forniés et al.[23a] The Pt−Pt distance is longer than those reported in the corresponding dimer $[Pt_2Cu_4(C{\equiv}CC_6H_5)_8]_2$[34] [3.116(2) Å] and the chains $[Pt_2Ag_4(C{\equiv}CC_6H_4OMe\text{-}3)_8]_\infty$ [3.1458(8) Å].[23a] The two clusters are rotated with a torsion angle C21−Pt1−Pt1A−C21B of 48.7°, but within each of the clusters **2**, the two square-planar $Pt(C{\equiv}CC_6H_5)_4$ fragments are found to be eclipsed. The Pt···Ag distances [3.1181(10) and 3.0957(11) Å] and Ag···Ag distance [3.0812(12) Å] are almost symmetrical, whereas the Ag−C bonds are asymmetrical, with Ag−C_α distances shorter than Ag−C_β bonds (Δ = 0.174−0.233 Å) and comparable to those found in **1**.

Photophysical Properties. The UV−vis spectra of complex **1** in different solvents were measured in solutions at room temperature (summarized in Table 1). The absorption spectra of dilute solutions of **1** show high-energy intraligand absorptions at 260−267 nm and two low-energy spin- and orbital-allowed bands at 345−362 and 374−400 nm, respectively, slightly red-shifted in relation to those of **2**. The low-energy band at 374−400 nm of **1** is unaffected by solvents

dx.doi.org/10.1021/ic3016657 | Inorg. Chem. 2012, 51, 11117−11125

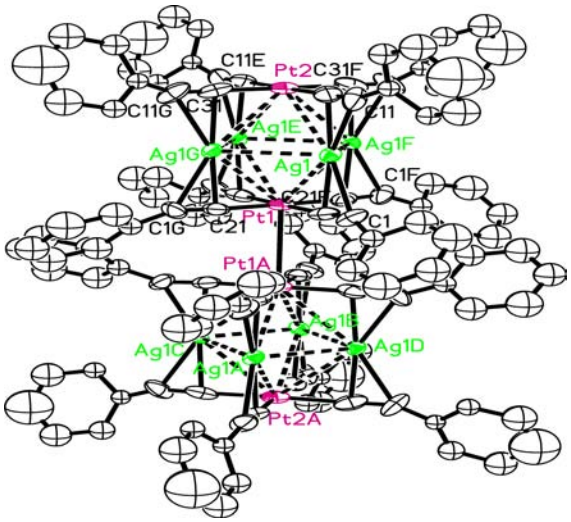

Figure 2. ORTEP view of **3** (molecule A) with 30% thermal ellipsoids.

Table 1. Photophysical Data for Compounds 1−3

compound	medium	λ_{abs}/nm (10^{-5} M) ($\varepsilon \times 10^5$/ dm^3 mol^{-1} cm^{-1})	λ_{em}/nm (τ_{em}/μs)[a] (298 K)	Φ_{em}[a]
1	solid		600 (4.35)	
	CH_2Cl_2	263 (0.98), 360 (0.23), 400 (0.28)	570 (1.54)	0.278[b]
	$ClCH_2CH_2Cl$	264 (1.37), 360 (0.33), 400 (0.39)	568 (1.15)	0.214[b]
	CH_3CN	264 (0.99), 360 (0.25), 400 (0.31)	566	0.003[b]
	THF	265 (1.07), 362 (0.26), 396 (0.27)	558	0.014[c]
2	solid		545 (3.04)[d]	
	CH_2Cl_2	263 (1.16), 357 (0.27), 393 (0.28)	562 (0.68)[d]	0.178[b]
	$ClCH_2CH_2Cl$	261 (0.97), 357(0.26), 392 (0.27)	562 (0.87)	0.186[b]
	CH_3CN	265 (0.65), 371 (0.17)	558	0.002[b]
	THF	263 (1.86), 361 (0.32), 390 (0.31)	548	0.007[c]
3	solid		655 (0.07)	

[a]The concentration of complexes **1** and **2** in different solutions is 1×10^{-4} M, and reported values were averaged from at least three measurements with a relative standard deviation of ~10%. [b]Measured using Rhodamine 6G as the standard. [c]Measured using $[Ru(bpy)_3]Cl_2$ as the standard. [d]Photophysical data reported in ref 23.

such as CH_2Cl_2, CH_2ClCH_2Cl, and methyl acetonitrile (MeCN) (400 nm) but is slightly blue-shifted (396 nm) in tetrahydrofuran (THF), which is similar to other reported hexanuclear clusters $[Pt_2Ag_4(C{\equiv}CR)_8]$ (R = Bu^t, C_6H_5, C_6H_4OMe-3, C_6H_4CN-4, $C_6H_4CF_3$-4, C_5H_4N-4, $C{\equiv}CC{\equiv}CC_6H_4CH_3$-4).[23,24] Following previous assignments,[23,24] these low-energy bands are attributed to MLM′CT (M = Pt; M′ = Ag) mixed with intraligand character.

With excitation λ_{ex} > 300 nm, cluster **1** emits strongly both in the solid state and in solution. The emission spectra of **1**−**3** in the solid state at room temperature are shown in Figure 3. As expected, the orange monomer **1** displays an intense red luminescence centered at 600 nm with a luminescence lifetime of 4.35 μs. The emission is notably red-shifted in relation to that of the previously reported monomer **2** (545 nm; τ = 3.04 μs),[23] which is consistent with the presence of the better electron-donating ability of the $C{\equiv}CC_6H_4CH_3$-4 ligand.

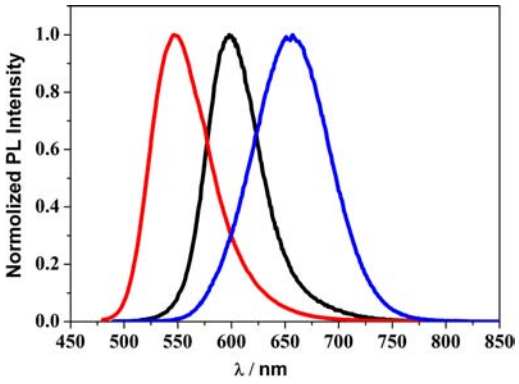

Figure 3. Emission spectra of complexes **1** (black line), **2** (red line), and **3** (blue line) in the solid state at room temperature.

Moreover, the quantum yields of **1** in the solid state and solution are higher than those of **2** (Table S3 in the Supporting Information). The crystalline and powdered samples of the red dimer **3** produce an intense red luminescence centered at 655 nm (τ = 0.07 μs), considerably red-shifted compared to the yellow monomer **2**, which is due to strong Pt···Pt interactions. In solution, as in the other reported hexanuclear clusters $[Pt_2Ag_4(C{\equiv}CR)_8]$ (R = Bu^t, C_6H_5, C_6H_4OMe-3, C_6H_4CN-4, $C_6H_4CF_3$-4, C_5H_4N-4, $C{\equiv}CC{\equiv}CC_6H_4CH_3$-4),[23,24] the luminescence of cluster **1** depends on the solvent and concentration. It is clear from Figure 4 that the emission

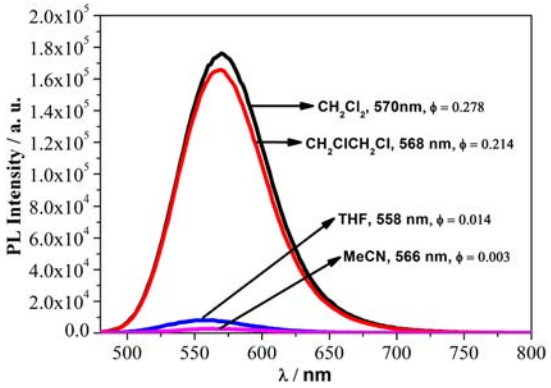

Figure 4. Emission spectra of **1** in 1×10^{-4} M CH_2Cl_2 (black line), CH_2ClCH_2Cl (red line), THF (blue line), and MeCN (magenta line) at room temperature, showing the different emission energies and quantum yields.

energy of **1** in different solvents (1×10^{-4} M) follows the order THF > MeCN > CH_2ClCH_2Cl > CH_2Cl_2, and the quantum yield follows the order CH_2Cl_2 (Φ = 0.278) > CH_2ClCH_2Cl (Φ = 0.214) > THF (Φ = 0.014) > MeCN (Φ = 0.003).

Interestingly, the transformation of the yellow monomer **2** and the red dimer **3** is reversible. As shown in Figure S2 in the Supporting Information, when crystals of the yellow monomer **2** were crushed, the red dimer **3** was obtained. Using the acetone to dissolve the red dimer **3**, the yellow suspended solution of monomer **2** was obtained. Furthermore, CH_2Cl_2/petroleum ether (1:5) was added to the above yellow suspended solution and evaporated in air; the red dimer **3** was obtained again. However, no similar behavior was found in the orange monomer **1**.

Electrochemistry. The redox behaviors of **1** and **2** (1×10^{-3} M) were determined by cyclic voltammetry in deaerated

dx.doi.org/10.1021/ic3016657 | Inorg. Chem. 2012, 51, 11117−11125

CH_2ClCH_2Cl (0.1 M Bu_4NPF_6) at a Pt electrode with a scan rate of 100 mV s^{-1}. For comparison, compounds $[NBu_4]_2[Pt(C{\equiv}CC_6H_4R\text{-}4)_4]$ (R = H, CH_3) have also been studied, and all electrochemical data are listed in Table 2.

Table 2. Electrochemical Data for Complexes 1, 2, and $[NBu_4]_2[Pt(C{\equiv}CC_6H_4R\text{-}4)_4]$ (R = H, CH_3)

	oxidation		reduction	
complex	E_{pa} (V)	E_{pc} (V)	E_{pa} (V)	E_{pc} (V)
1	+0.81, +1.00		−0.19	−1.34
2	+0.83, +1.04		−0.17	−1.37
$[NBu_4]_2[Pt(C{\equiv}CC_6H_4CH_3\text{-}4)_4]$	+0.55			−1.79
$[NBu_4]_2[Pt(C{\equiv}CC_6H_5)_4]$	+0.60			−1.82

The precursor $[NBu_4]_2[Pt(C{\equiv}CC_6H_4R\text{-}4)_4]$ (R = H, CH_3) shows one irreversible reduction wave, which is assigned to the reduction of the alkynyl ligand $C{\equiv}CC_6H_4R$-4 (R = H, CH_3), and one irreversible oxidation wave from the platinum(II)/platinum(III) redox reaction (shown in Figure S3 in the Supporting Information). The reduction potential for $[NBu_4]_2[Pt(C{\equiv}CC_6H_4CH_3\text{-}4)_4]$ at −1.79 V is less negative than that of $[NBu_4]_2[Pt(C{\equiv}CC_6H_5)_4]$ at −1.82 V, and the oxidation potential for $[NBu_4]_2[Pt(C{\equiv}CC_6H_4CH_3\text{-}4)_4]$ at 0.55 V is less positive than that of $[NBu_4]_2[Pt(C{\equiv}CC_6H_5)_4]$ at 0.60 V, which is due to a better electron-donating ability of the alkynyl ligand $C{\equiv}CC_6H_4CH_3$-4 than that of the ligand $C{\equiv}CC_6H_5$.

As shown the CVs in Figure 5, **1** and **2** undergo two irreversible reduction processes at −0.19 and −1.34 V for **1** and

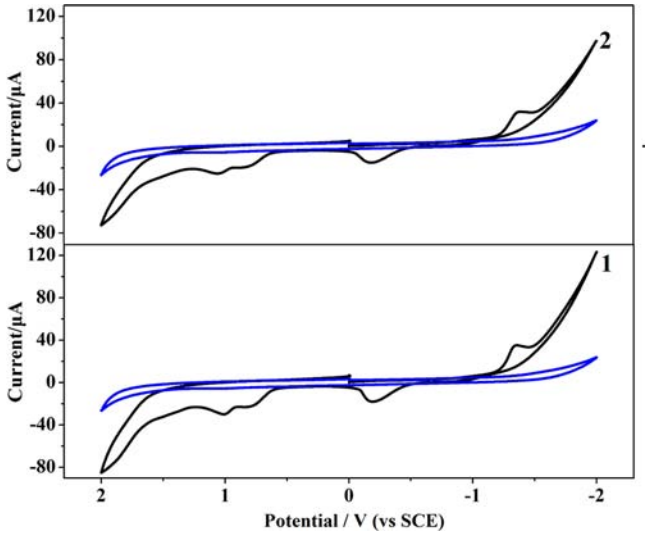

Figure 5. CVs of 1 mM **1** and **2** in deaerated CH_2ClCH_2Cl (0.1 M Bu_4NPF_6) at a Pt electrode. Scan rate = 100 mV s^{-1}. The blue lines represent the CVs in the blank solution under the same experimental conditions.

at −0.17 and −1.37 V for **2**, respectively, which are very different from the reduction processes in the CVs of the precursor $[NBu_4]_2[Pt(C{\equiv}CC_6H_4R\text{-}4)_4]$ (R = H, CH_3; shown in Figure S3 in the Supporting Information). Following previous assignments,[24] the irreversible reduction waves for **1** and **2** are ascribed to the reduction of the silver atom. In the anodic region, two irreversible oxidation waves are observed at 0.81 and 1.00 V for **1** and 0.83 and 1.04 V for **2**, respectively. On the basis of the fact that only one irreversible oxidation wave is observed in the CV of the precursor $[NBu_4]_2[Pt(C{\equiv}CC_6H_4R\text{-}4)_4]$ (R = H, CH_3), two irreversible oxidation waves in the CVs of **1** and **2** are assigned to the oxidation of two platinum atoms. Furthermore, the irreversible nature of the oxidation wave in the CVs of **1** and **2** indicates the instability of the oxidation products of **1** and **2** due to a fast decomposition process. The oxidation potentials of **1** are less positive than those of **2**, which is due to a better electron-donating ability of the alkynyl ligand $C{\equiv}CC_6H_4CH_3$-4 than that of $C{\equiv}CC_6H_5$.

The dependences of the anodic peak currents of **1** and **2** were investigated to identify the type of current over the range of scan rates from 10 to 300 mV s^{-1}. With an increase of the scan rate, two reduction peak currents of **1** and **2** are increased markedly and are both proportional to the square root of the scan rate, which indicates that the electrochemical processes are controlled by diffusion (shown in Figure S4 in the Supporting Information).

ECL. No ECL emissions of **1** and **2** associated with radical-ion annihilation were observed when the potential was pulsed between the oxidation and reduction waves of **1** and **2** (∼+2.0 and −2.0 V). The result is similar to that found in the alkynylgold(III) complex[8a] but distinctly in contrast to the intense ECL emissions observed for $[Ru(bpy)_3]^{2+}$ and its derivatives.[2−6]

The coreactant system ECL also has been studied using 50 μM **1** or **2** with different amine coreactants (TPrA or DBAE), in different solvents (CH_2Cl_2, CH_2ClCH_2Cl, or CH_3CN), at different working electrodes (GC, Au, or Pt). It is found that the experimental conditions, such as the nature of the solvent, electrode materials, and coreactants could influence the ECL of **1** and **2** to different extents.

Interestingly, the effect of the nature of the solvent on the ECL was very different from that on the PL. It was found that strong ECL emissions were found in CH_2Cl_2 and CH_2ClCH_2Cl solutions of **1** or **2** in the presence of amine coreactants (TPrA and DBAE), while no ECL signals were detected in a MeCN solution of **1** or **2** in the presence of amine coreactants (TPrA and DBAE). ECL of **1**- and **2**/amine systems in CH_2Cl_2 is unstable because of the volatility of the CH_2Cl_2 solvent; therefore, ECL of **1**- and **2**/amine systems was investigated in CH_2ClCH_2Cl.

ECL of **1** or **2** in CH_2ClCH_2Cl in the presence of amine coreactants (TPrA and DBAE) was also investigated at different working electrodes (GC, Au, or Pt), shown in Figure 6. It is noted that the ECL intensities and potentials of the **1**/amine system depend on the electrode materials. As shown in Figure 6, among Pt, Au, and GC working electrodes, the ECL intensity of **1**/TPrA or DBAE system in CH_2ClCH_2Cl solutions at different working electrodes follows the order Pt electrode > Au electrode > GC electrode. When the potential was scanned positively close to 0.83 V, the ECL signals of the **1**/DBAE system were observed and reached maximum intensity at potentials of 1.14 V at Pt and Au electrodes and 1.25 V at GC electrodes. However, in the **1**/TPrA system, the ECL signals appeared at 0.70 V and reached maximum intensity at potentials of 1.16 V at Pt electrode, 1.10 V at Au electrode, and 0.94 V at GC electrode, respectively. Similar results were also obtained in the **2**/TPrA or DBAE system.

It is noted that the ECL intensities of **1** and **2** in CH_2ClCH_2Cl depend on the concentration of the amine coreactants at a Pt working electrode. Figure 7 shows the ECL

dx.doi.org/10.1021/ic3016657 | Inorg. Chem. 2012, 51, 11117−11125

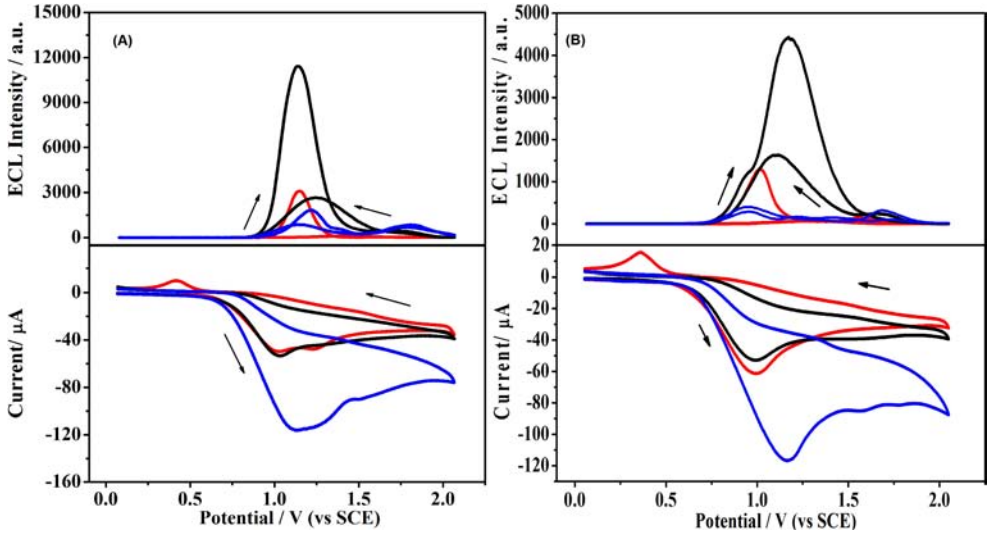

Figure 6. CVs and corresponding ECL curves of 50 μM **1** in deaerated CH_2ClCH_2Cl (0.1 M Bu_4NPF_6) at Pt (black line), Au (red line), and GC (blue line) working electrodes with 15 mM DBAE (A) or TPrA (B) as the coreactant. Scan rate = 100 mV s^{-1}.

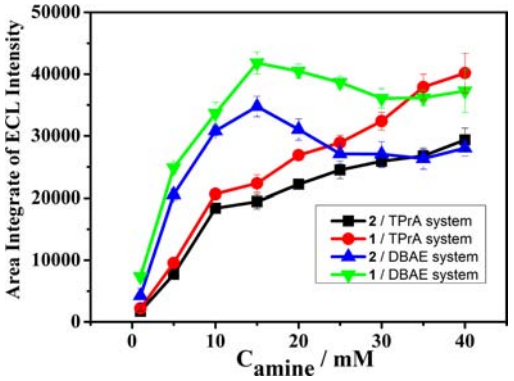

Figure 7. ECL intensity changes of 50 μM **1** and **2** with different concentrations of the amine coreactants at a Pt working electrode.

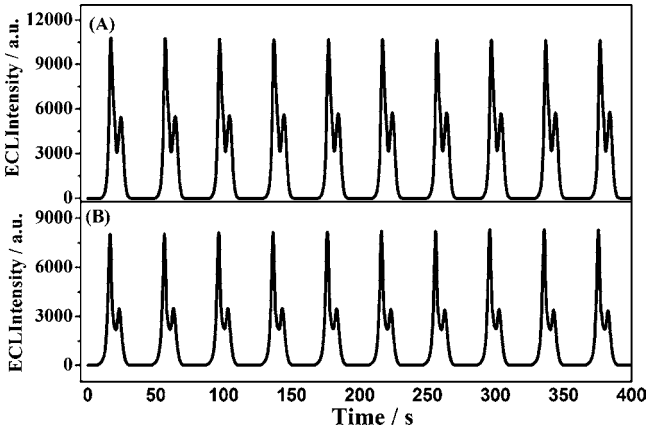

Figure 8. ECL stability of the **1** (A) and **2** (B) (50 μM)/DBAE (15 mM) systems in CH_2ClCH_2Cl. The potential was scanned from 0 to 2.0 V with a scan rate of 100 mV s^{-1}.

intensity changes of 50 μM **1** and **2** in CH_2ClCH_2Cl with different concentrations of TPrA and DBAE. The ECL intensities of **1** and **2** are pronounced, increasing with the increasing concentration of TPrA, while the ECL intensities of **1** and **2** increase rapidly with increasing DBAE concentration up to 15 mM and then decrease slowly upon further increasing DBAE concentration. The ECL intensity changes of **1** and **2** with different amine (TPrA and DBAE) concentrations are in accordance with those found in the $[Ru(bpy)_3]^{2+}$/amine coreactant system.[2−6] With the same TPrA or DBAE concentration, the ECL intensity of **1** is stronger than that of **2**, and the ECL intensities of the **1**- and **2**/DBAE systems are both higher than those of the TPrA system.

ECL of the **1**- and **2**/amine (TPrA and DBAE) systems in CH_2ClCH_2Cl at a Pt working electrode is very stable. When the potential is scanned from 0 to 2.0 V for 10 times, the ECL signals of the **1**- and **2**/DBAE systems are almost unchanged (shown in Figure 8), indicating these new ECL systems could be expected to apply in analytical areas.

Under the same experimental conditions, the potentials of the maximum ECL intensity of the **1**/amine system are slightly shifted by about 0.03 V toward more negative potential than those of the **2**/amine system, which is consistent with that obtained by cyclic voltammogram scans, as shown Figure 9. As a comparison, ECL curves of the same $Ru(bpy)_3^{2+}$/amine system were recorded. The comparison of Figure 9 clearly indicates that the ECL potentials of the **1**- and **2**/amine systems are notably negatively shifted by about 0.38 V compared to those of the $Ru(bpy)_3^{2+}$/amine system.

ECL quantum efficiencies of the **1**- and **2**/amine coreactant systems in CH_2ClCH_2Cl were measured using $[Ru(bpy)_3](PF_6)_2$ (φ°_{ECL} = 1) as the standard.[31] Under the same experimental conditions, ECL quantum efficiencies of the **1**/amine system (φ°_{ECL} = 0.36 for the **1**/TPrA system and 0.57 for the **1**/DBAE system, respectively) are higher than those of the **2**/amine system (φ°_{ECL} = 0.29 for the **2**/TPrA system and 0.48 for the **2**/DBAE system, respectively), which are on the same order of magnitude as that of the $[Ru(bpy)_3](PF_6)_2$/amine system.

ECL Mechanism. It is clear from Figure S5 in the Supporting Information that the ECL spectra of the **1**/TPrA system are almost identical with their PL spectra, indicating that the emissive states f **1** generated in the ECL experiment may also be derived from a MLM′CT [Pt(d)/π (C≡CC_6H_4R-4) → Pt(p_z)/Ag(sp) /π^*(C≡CC_6H_4R-4)] state modified by Pt···Ag and Ag···Ag contacts. In analogy with the known $[Ru(bpy)_3]^{2+}$/

dx.doi.org/10.1021/ic3016657 | Inorg. Chem. 2012, 51, 11117−11125

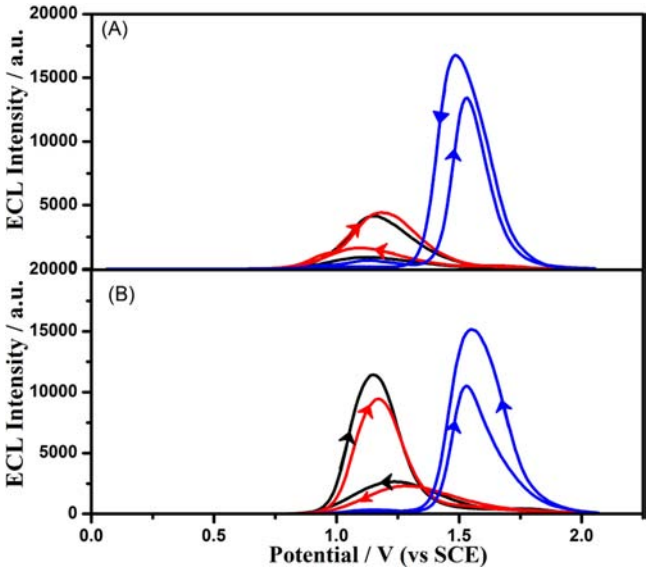

Figure 9. ECL curves of 50 μM **1** (black line), **2** (red line), and $Ru(bpy)_3^{2+}$ in deaerated CH_2ClCH_2Cl (0.1 M Bu_4NPF_6) at a Pt working electrode with 15 mM TPrA (A) or DBAE (B) as the coreactant. Scan rate = 100 mV s^{-1}.

TPrA system, ECL generation from **1** could be explained by the following reaction:

$$\mathbf{1} - e^- \rightarrow \mathbf{1}^+ \quad (1)$$

$$TPrA - e^- \rightarrow TPrA^\bullet + H^+ \quad (2)$$

$$\mathbf{1}^+ + TPrA^\bullet \rightarrow \mathbf{1}^{+}* + P_1 \quad (3)$$

$$\mathbf{1}^{+}* \rightarrow \mathbf{1}^+ + h\nu \quad (4)$$

where $TPrA^\bullet$ is $(CH_3CH_2CH_2)_2NC^\bullet HCH_2CH_3$ and P_1 is $Pr_2N^+{=}CHCH_2CH_3$. In order to predict where eq 3 is sufficiently energetic to generate the excited state, we estimate the energy $(-\Delta H)$ available in the reaction by employing the following equation:[1c]

$$-\Delta H = E^\circ(1 + /1) - E^\circ(P_1/TPrA^\bullet) - 0.1 \text{ eV } (1) \quad (5)$$

where 0.1 eV is the entropy approximation term (TDS°) at 25 °C and the redox potentials (vs NHE) of $\mathbf{1}^+/\mathbf{1}$ and $P_1/TPrA^\bullet$ are 1.11 and −1.5 V, respectively.[1c] The estimated $-\Delta H$ is 2.51 eV, which is much higher than the energy of $\mathbf{1}^{+}*$ (2.18 eV). This indicates that the reducing activity of $TPrA^\bullet$ is strong enough to reduce $\mathbf{1}^+$ directly into $\mathbf{1}^{+}*$, giving the ECL emission. The same ECL mechanism is ascribed to the **2**/TPrA system.

Determination of Sudan I. It is noted that the ECL intensity of the **1**/amine coreactant (TPrA or DBAE) system in CH_2ClCH_2Cl (0.1 M Bu_4NPF_6) at a Pt working electrode is quenched by Sudan I, but the CVs of the **1**/amine coreactant system were not changed in the presence of Sudan I, as shown in Figure S6 in the Supporting Information. Figure 10 shows the ECL changes of 20 μM **1** in CH_2ClCH_2Cl (0.1 M Bu_4NPF_6) including 15 mM DBAE with different concentrations of Sudan I at a Pt working electrode. The ECL intensity of the **1**/DBAE system was decreased with increasing Sudan I concentration. The quenched ratio of the area integrations of the ECL intensity $[(I_0 - I)/I_0]$ was linear with the logarithm of the Sudan I concentration ($C_{Sudan\ I}$) in the range of 2.5×10^{-5}–1.0×10^{-3} M. The regression equation was

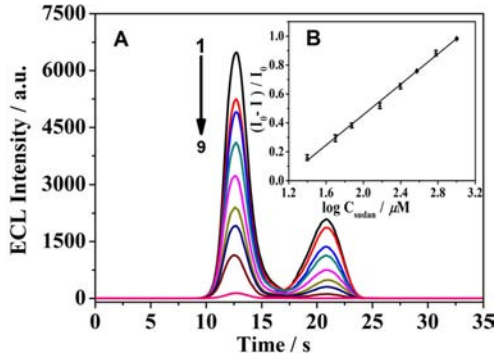

Figure 10. (A) ECL curves of 20 μM **1** in CH_2ClCH_2Cl (0.1 M Bu_4NPF_6) including 15 mM DBAE at a Pt working electrode with different concentrations of Sudan I from 1 to 9: 0, 2.50×10^{-5}, 5.00×10^{-5}, 7.50×10^{-5}, 1.50×10^{-4}, 2.50×10^{-4}, 3.75×10^{-4}, 6.00×10^{-4}, and 1.00×10^{-3} M. (B) Plot of $[(I_0 - I)/I_0]$ versus the concentration of Sudan I. I_0 and I are the area integrations of the logarithm of ECL intensity of the **1**/DBAE system without and with Sudan I.

$$(I_0 - I)/I_0 = -0.5982 + 0.5269 \log C_{Sudan\ I},$$
$$R^2 = 0.9931$$

where I_0 and I are the area integrations of the ECL intensity of the **1**/DBAE system in the absence and presence of Sudan I and R is the regression coefficient. A detection limit for Sudan I was 8.0×10^{-6} M based on 3 times the ratio of signal-to-noise, compared to the reported determination methods.[15–22]

In order to estimate the interaction between complex **1** and Sudan I, the UV–vis and PL spectra of 20 μM complex **1** in CH_2ClCH_2Cl in the absence and presence of Sudan I were also investigated as shown in Figures S7 and S8 in the Supporting Information. It is found that the PL intensity of complex **1** in CH_2ClCH_2Cl is also quenched by Sudan I, and the quenched ratio $[(F_0 - F)/F_0]$ was also linear with the logarithm of the Sudan I concentration ($C_{Sudan\ I}$) in the range of 2.5×10^{-5}–1.0×10^{-3} M. However, the UV–vis spectrum of the **1**/Sudan I system was the simple sum of the individuals of complex **1** and Sudan I, which indicated that no new compounds were produced by the simple mixing of complex **1** and Sudan I. It is worthwhile to note that Sudan I exhibits a broad absorption band at 350–550 nm, which is partly overlapped with the emission band of cluster **1**. Therefore, we inferred that the ECL and PL quenching by Sudan I was perhaps due to the energy transfer from the emission state of cluster **1** to Sudan I.

■ CONCLUSIONS

Two hexanuclear monomers $[Pt_2Ag_4(C{\equiv}CC_6H_4R)_8]$ (R = CH_3, **1**; R = H, **2**), together with dimer **3**, have been synthesized by the self-assembly reaction of $[NBu_4]_2[Pt(C{\equiv}CC_6H_4R\text{-}4)_4]$ and $[Ag_2(\mu\text{-dppy})_2](ClO_4)_2$ (dppy = 2-(diphenylphosphino)pyridyl) and characterized. Their PL properties and electrochemical and ECL characteristics in the absence/presence of coreactant TPrA or DBAE at different working electrodes in different solvents (CH_2Cl_2, CH_2ClCH_2Cl, or CH_3CN) have also been investigated. Monomers **1** and **2** in CH_2ClCH_2Cl solutions were first found to exhibit intense ECL emissions using amine (TPrA and DBAE) as the coreactant at a Pt working electrode. The ECL potentials of **1** and **2** in CH_2ClCH_2Cl solutions were at 1.14–1.19 V vs SCE, significantly negatively shifted by about 0.38 V compared to those of the $Ru(bpy)_3^{2+}$/amine system. In all

dx.doi.org/10.1021/ic3016657 | Inorg. Chem. 2012, 51, 11117–11125

cases, the ECL quantum efficiencies of **2** are higher than those of **1** and on the same order of magnitude as that of the $[Ru(bpy)_3](PF_6)_2$/amine system. Interestingly, it is found that Sudan I will quench the ECL intensity of the **1**/DBAE system in CH_2ClCH_2Cl solutions at a Pt working electrode, and a mechanism of quenching ECL was proposed. Therefore, a new ECL method for the determination of Sudan I was developed with a linear range of 2.5×10^{-5}–1.0×10^{-3} M and a detection limit of 8.0×10^{-6} M based on 3 times the ratio of signal-to-noise.

■ ASSOCIATED CONTENT

Supporting Information

Crystallographic parameters and details for data collections and refinements of compounds **1** and **3**, X-ray crystallographic file in CIF format for the structure determination of compounds **1** and **3**, and Figures S1–S8. This material is available free of charge via the Internet at http://pubs.acs.org.

■ AUTHOR INFORMATION

Corresponding Author

*E-mail: qhw76@fzu.edu.cn (Q.-H.W.), gnchen@fzu.edu.cn (G.-H.C.).

Notes

The authors declare no competing financial interest.

■ ACKNOWLEDGMENTS

This study was financially supported by the National Nature Sciences Foundation of China (Grant 20801013), the National Basic Research Program of China (Grant 2010CB732403), Fuzhou University (Grant XRC-0723), Key Science Project (type A) of the Fujian Provincial Department of Education, China (Grant JA12021), and the Program for Changjiang Scholars and Innovative Research Team in University (Grant IRT1116).

■ REFERENCES

(1) (a) Bard, A. J., Ed. *Electrogenerated Chemiluminescence*; Dekker: New York, 2004. (b) Bard, A. J.; Faulkner, L. R. *Electrochemical Methods: Fundamentals and Application*, 2nd ed.; John Wiley and Sons: New York, 2000; Chapter 6. (c) Richter, M. M. *Chem. Rev.* **2004**, *104*, 3003. (d) Miao, W. J. *Chem. Rev.* **2008**, *108*, 2506. (e) Hu, L. Z.; Xu, G. B. *Chem. Soc. Rev.* **2010**, *39*, 3275.

(2) (a) Miao, W. J.; Bard, A. J. *Anal. Chem.* **2004**, *76*, 7109. (b) Zu, Y. B.; Bard, A. J. *Anal. Chem.* **2000**, *72*, 3223. (c) Miao, W. J.; Bard, A. J. *Anal. Chem.* **2003**, *75*, 5825. (d) Stagni, S.; Palazzi, A.; Zacchini, S.; Ballarin, B.; Bruno, C.; Marcaccio, M.; Paolucci, F.; Monari, M.; Carano, M.; Bard, A. J. *Inorg. Chem.* **2006**, *45*, 695.

(3) (a) Zhou, M.; Robertson, G. P.; Roovers, J. *Inorg. Chem.* **2005**, *44*, 8317. (b) Nickita, N.; Gasser, G.; Pearson, P.; Belousoff, M. J.; Goh, L. Y.; Bond, A. M.; Deacon, G. B.; Spiccia, L. *Inorg. Chem.* **2009**, *48*, 68.

(4) Wei, Q. H.; Lei, Y. F.; Duan, Y. N.; Xiao, F. N.; Li, M. J.; Chen, G. N. *Dalton Trans.* **2011**, *40*, 11636.

(5) (a) Wightman, R. M.; Forry, S. P.; Maus, R.; Badocco, D.; Pastore, P. *J. Phys. Chem. B* **2004**, *108*, 19119. (b) Zorzi, M.; Pastore, P.; Magno, F. *Anal. Chem.* **2000**, *72*, 4934.

(6) (a) Wei, H.; Yin, J. Y.; Wang, E. K. *Anal. Chem.* **2008**, *80*, 5635. (b) Yin, X. B.; Dong, S. J.; Wang, E. K. *TrAC, Trends Anal. Chem.* **2004**, *23*, 432. (c) Wei, H.; Du, Y.; Kang, J. Z.; Wang, E. K. *Electrochem. Commun.* **2007**, *9*, 1474.

(7) Wei, Q. H.; Xiao, F. N.; Han, L. J.; Zeng, S. L.; Duan, Y. N.; Chen, G. N. *Dalton Trans.* **2011**, *40*, 5078.

(8) (a) Chen, Z. F.; Wong, K. M.-C.; Au, V. K.-M.; Zu, Y. B.; Yam, V. W.-W. *Chem. Commun.* **2009**, 791. (b) Chen, Z. F.; Wong, K. M.-C.; Kwok, E. C.-H.; Zhu, N. Y.; Zu, Y. B.; Yam, V. W.-W. *Inorg. Chem.* **2011**, *50*, 2125.

(9) (a) Lang, H.; del Villar, A. *J. Organomet. Chem.* **2003**, *670*, 45. (b) Berenguer, J. R.; Lalinde, E.; Moreno, M. T. *Coord. Chem. Rev.* **2010**, *254*, 832.

(10) (a) Yam, V. W.-W. J. *Organomet. Chem.* **2004**, *689*, 1393. (b) Wong, K. M.-C.; Hui, C.-K.; Yu, K.-L.; Yam, V.W.-W. *Coord. Chem. Rev.* **2002**, *229*, 123. (c) Yam, V. W.-W. *Acc. Chem. Res.* **2002**, *35*, 555. (d) Yam, V. W.-W.; Lo, K. K. W.; Wong, K. M. C. *J. Organomet. Chem.* **1999**, *578*, 3.

(11) Chen, Z. N.; Zhao, N.; Fan, Y.; Ni, J. *Coord. Chem. Rev.* **2009**, *253*, 1.

(12) (a) Hissler, M.; McGarrah, J. E.; Connick, W. B.; Geiger, D. K.; Cummings, S. D.; Eisenberg, R. *Coord. Chem. Rev.* **2000**, *208*, 115. (b) Ziessel, R.; Hissler, M.; El-ghayoury, A.; Harriman, A. *Coord. Chem. Rev.* **1998**, *178–180*, 1251.

(13) Refat, N. A. G. A.; Ibrahim, Z. S.; Moustafa, G. G.; Sakamoto, K. Q.; Ishizuka, M.; Fujita, S. *J. Biochem. Mol. Toxicol.* **2008**, *22*, 77.

(14) European Commission. Health and Consumer Protection Directorate General, Committee IV—Food Safety in Production and Currency, Part III—Physical and Chemical Substances Surveillance, New Method Declaration, March 1999.

(15) Wang, S.; Xu, Z. X.; Fang, G. Z.; Duan, Z. J. *J. Agric. Food Chem.* **2007**, *55*, 3869.

(16) Murty, M. R. V. S.; Chary, N.-S.; Prabhakar, S.; Raju, N.-P.; Vairamani, M. *Food Chem.* **2009**, *115*, 1556.

(17) Zhang, Y.; Wu, H. L.; Xia, A. L.; Han, Q. J.; Cui, H.; Yu, R. Q. *Talanta* **2007**, *72*, 926.

(18) Zhang, Y. T.; Zhang, Z. J.; Sun, Y. H. *J. Chromatogr. A* **2006**, *1129*, 34.

(19) (a) Yin, H. S.; Zhou, Y. L.; Meng, X. M.; Tang, T. T.; Ai, S. Y.; Zhu, L. S. *Food Chem.* **2011**, *127*, 1348. (b) Chen, S. Z.; Du, D.; Huang, J.; Zhang, A. Q.; Tu, H. Y.; Zhang, A. D. *Talanta* **2011**, *84*, 451.

(20) (a) Zhang, Z.; Xu, S. F.; Li, J. H.; Xiong, H.; Peng, H. L.; Chen, L. X. *J. Agric. Food Chem.* **2012**, *60*, 180. (b) Yan, H. Y.; Qiao, J. D.; Pei, Y. N.; Long, T.; Ding, W.; Xie, K. *Food Chem.* **2012**, *132*, 649.

(21) Wu, L. P.; Li, Y. F.; Huang, C. Z.; Zhang, Q. *Anal. Chem.* **2006**, *78*, 5570.

(22) Wang, Y. Z.; Yang, H.; Wang, B.; Deng, A.-P. *J. Sci. Food Agric.* **2011**, *91*, 1836.

(23) (a) Gil, B.; Forniés, J.; Gómez, J.; Lalinde, E.; Martín, A.; Moreno, M. T. *Inorg. Chem.* **2006**, *45*, 7788. (b) Ara, I.; Forniés, J.; Gómez, J.; Lalinde, E.; Moreno, M. T. *Organometallics* **2000**, *19*, 3137. (c) Benito, J.; Berenguer, J. R.; Forniés, J.; Gil, B.; Gómez, J.; Lalinde, E. *Dalton Trans.* **2003**, 4331. (d) Espinet, P.; Forniés, J.; Martínez, F.; Tomás, M.; Lalinde, E.; Moreno, M. T.; Ruiz, A.; Welch, A. J. *J. Chem. Soc., Dalton Trans.* **1990**, 791.

(24) Yam, V. W.-W.; Hui, C. K.; Yu, S. Y.; Zhu, N. *Inorg. Chem.* **2004**, *43*, 812.

(25) Kuang, S. M.; Zhang, L. M.; Zhang, Z. Z.; Wu, B. M.; Mak, T. C. W. *Inorg. Chim. Acta* **1999**, *284*, 278.

(26) (a) Evans, P. R. *Proceedings of the CCP4 Study Weekend. Recent Advances in Phasing*; Wilson, K. S., Davies, G., Ashton, A. W., Bailey, S., Eds.Daresbury Laboratory: Warrington, U.K., 1997. (b) Sheldrick, G. M. *SHELXL-97, Program for the Refinement of Crystal Structures*; University of Göttingen: Göttingen, Germany, 1997.

(27) Eaton, D. F. *Pure Appl. Chem.* **1988**, *60*, 1107.

(28) Houten, J.; Van Watts, R. J. *J. Am. Chem. Soc.* **1976**, *98*, 4853.

(29) Wu, X. P.; Huang, F. X.; Duan, J. P.; Chen, G. N. *Talanta* **2005**, *65*, 1279.

(30) Masui, M.; Sayo, H.; Tsuda, Y. *J. Chem. Soc. B* **1968**, 973.

(31) Richter, M. M.; Debad, J. D.; Striplin, D. R.; Crosby, G. A.; Bard, A. J. *Anal. Chem.* **1996**, *68*, 4370.

(32) (a) Ara, I.; Berenguer, J. R.; Eguizábal, E.; Forniés, J.; Lalinde, E. *Organometallics* **2001**, *20*, 2686. (b) Ara, I.; Forniés, J.; Gómez, J.; Lalinde, E.; Merino, R. I.; Moreno, M. T. *Inorg. Chem. Commun.* **1999**, *2*, 62.

(33) (a) Wei, Q. H.; Yin, G. Q.; Ma, Z.; Shi, L. X.; Chen, Z. N. *Chem. Commun.* **2003**, 2188. (b) Yin, G. Q.; Wei, Q. H.; Zhang, L. Y.; Chen, Z. N. *Organometallics* **2006**, *25*, 580.
(34) Yam, V. W.-W.; Yu, K. L.; Cheung, K.-K. *J. Chem. Soc., Dalton Trans.* **1999**, 2913.